Electronic Supplementary Information

Fabrication of Hierarchical Rh Nanostructures by Understanding the Growth Kinetics of Facet-controlled Rh Nanocrystals

Heonjo Kim,[a] Nguyen Tien Khi,[a] Jisun Yoon,[a] Hongseok Yang,[a] Youngjoo Chae,[a] Hionsuck Baik,[b] HyunKyung Lee,[c] Jeong-Hun Sohn,[c] Kwangyeol Lee[a*]*

[a] Department of Chemistry and Research Institute for Natural Sciences, Korea University, Seoul, 136-701 (Korea)
[b] Korea Basic Science Institute (KBSI), Seoul, 136-713(Korea)
[c] Department of Chemistry, Chungnam National University, Daejeon, 305-764 (Korea)

Material characterization

Transmission electron microscopy (TEM) and high-resolution TEM were performed on a TECNAI G2 20 S –Twin operated at 200 kV and a TECNAI G2 F30 operated at 300 kV. X-ray diffraction (XRD) patterns were collected with a Rigaku Ultima III diffractometer system using a graphite-monochromatized Cu-Kα radiation at 40 kV and 30 mA. Gas chromatography equipped with Mass spectroscopy (GC-MS) by using Clarus 600 series and Turbomatrix HSS Trap was used to analyze organic compounds in the catalysis. Inductively coupled plasma atomic emission spectroscopy (ICP-AES) data were collected with Ultima 2C.

Experimental Section

Preparation of Rh nanotetrahedrons (Fig. 1a) : A slurry of Rh(acac)$_3$ (0.05 mmol, Strem, 99%), 1,2-hexadecanediol (0.93 mmol, Aldrich, 90%) and stearic acid (0.037 mmol, Aldrich, 95%) in 1-octadecene (3 mL, Aldrich, 90%) was prepared in a two-neck round bottom flask (15 mL) with a magnetic stirring. After being evacuated for 25 min with stirring at 100 ^{o}C, the resulting solution was heated up to 245 ^{o}C at a heating rate of 5 ^{o}C/min, **and kept at that temperature for 30 min under slow O$_2$/Ar mixture gas flow** (5% v/v in Ar, 1 atm, 2 cc/min)**.** Dark brown precipitates were obtained by cooling down the solution to room temperature and then by centrifugation with added methanol/toluene (v/v = 2/5 mL).

Preparation of Rh tetrahedral nanoframes (Fig. 1c) : The method to obtain Rh tetrahedral nanoframe is similar to the preparation of Rh tetrahedron nanoparticle, except for the amount of stearic acid (0.075 mmol, Aldrich, 95%) and the heating condition (heated to 265 ^{o}C at a heating rate of 5 ^{o}C/min, **and kept at that temperature for 1 h).**

Preparation of Rh nanotetrapods (Fig. 1e) : A mixture of Rh(acac)$_3$ (0.05 mmol, Strem, 99%), 1,2-hexadecanediol (0.93 mmol, Aldrich, 90%) and octadecylamine (15 mmol, Aldrich, technical grade, 90%) was prepared in a two-neck round bottom flask (15 mL) at 90 ^{o}C with a magnetic stirring. After being evacuated for 25 min with stirring at 90 ^{o}C, the resulting

solution was heated up to 130 $^\circ$C **and kept at that temperature for 14 h under slow Ar flow** (99.9%, 2 cc/min)**.** Dark brown precipitates were obtained by cooling down the solution to room temperature and then by centrifugation with added methanol/toluene (v/v = 3/3).

Branch growth from Rh nanotetrahedron core (Fig. S10) : Rh nanotetrahedrons (3 mg) were dispersed in a mixture of Rh(acac)$_3$ (0.05mmol, Strem, 99%), 1,2-hexadecanediol (0.93 mmol, Aldrich, 90%) and octadecylamine (15 mmol, Aldrich, technical grade, 90%) in a two-neck round bottom flask (15 mL) with a magnetic stirring at 90 $^\circ$C. After being evacuated for 5 min with stirring at 90 $^\circ$C, the resulting solution was heated up to 130 $^\circ$C and kept at that temperature for 14 h under slow Ar gas flow (99.9%, 2 cc/min). Dark brown precipitates were obtained by cooling down the solution to room temperature and then by centrifugation with added methanol/toluene (v/v = 3/3 mL).
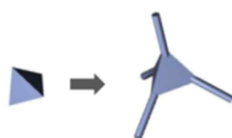
Growth of tetrahedral tips on the branches grown out from a tetrahedral core (Fig. 2b) : The method to form the tetrahedral Rh nanostructures is similar to the branch growth from Rh nanotetrahedron cores, except for the type of seed and its amount (Branched Rh nanotetrahedron core, 9 mg).
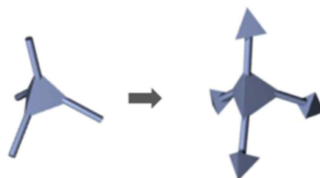
Branch growth from 16 corners of tetrahedral tips from a tetrahedral core (Fig. 2c) : The branch growth from 16 corners of dagger-shaped tips was similar to the preparation of branch growth from Rh nanotetrahedron cores, except for using a different kind of seed (nanostructure shown in Fig. 3b).
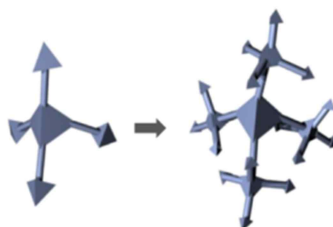
Branch growth from Rh tetrahedral nanoframes (Fig. 2f) : Rh nanoframes (3 mg) were dispersed in a mixture of Rh(acac)$_3$ (0.05 mmol, Strem, 99%), 1,2-hexadecanediol (0.93 mmol, Aldrich, 90%) and octadecylamine (15 mmol, Aldrich, technical grade, 90%) in a two-neck round bottom flask (15 mL) with a magnetic stirring at 90 ^{o}C. After being evacuated for 5 min with stirring at 90 ^{o}C, the resulting solution was heated up to 130 ^{o}C and kept at that temperature for 14 h under slow Ar gas flow (99.9%, 2 cc/min). Dark brown precipitates were obtained by cooling down the solution to room temperature and then by centrifugation with added methanol/toluene (v/v = 3/3 mL).

Further branch growth from tips on the branches grown out from a Rh nanoframe (Fig. 2g) : The branch growth from 16 corners of pyramid-shaped tips was similar to the preparation of branch growth from Rh nanoframe, except for using a different kind of seed (branched Rh nanoframe (Fig. 3f).
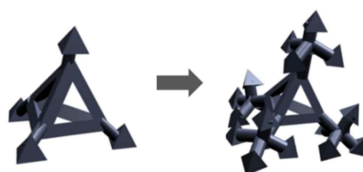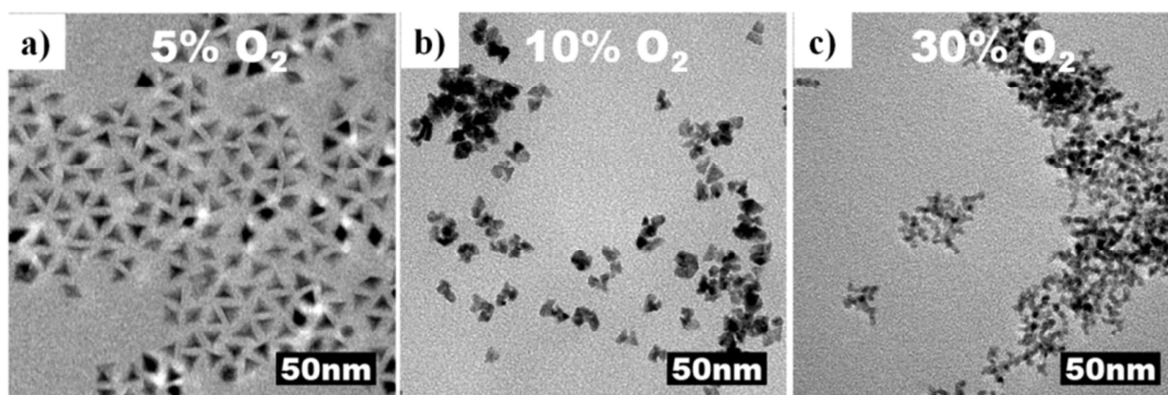
Fig. S1 The effect of the concentration of oxygen gas on the formation of Rh nanotetrahedrons. **a,** TEM image of Rh nanotetrahedrons; 5% oxygen in mixture gas. **b,** TEM image of various shaped Rh nanostructures; 10% oxygen in mixture gas. **c,** TEM image of Rh dendritic nanostructures; 30% oxygen in mixture gas. The reaction condition was similar to that for the preparation of Rh nanotetrahedrons except the concentration of **oxygen in mixture gas.**
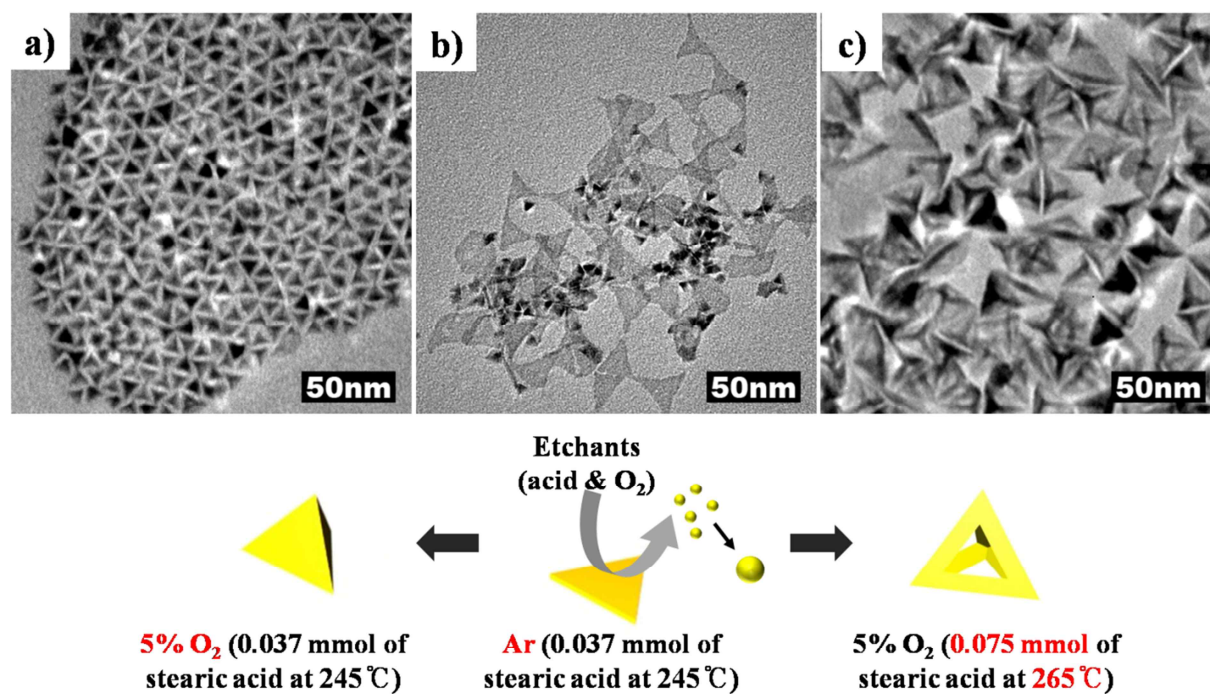
Fig. S2 The etchants such as organic acid and oxygen can remove unstable Rh nanoplates and drive the reaction to form nanotetrahedrons or nanoframes selectively. **a,** TEM image of Rh nanotetrahedrons. **b**, TEM image of small Rh nanotetrahedrons and Rh sheets. **c**, TEM image of Rh nanoframe. **d**, schematic diagram of the effect of oxidative etchants such as the amount of acids and the concentration of oxygen.
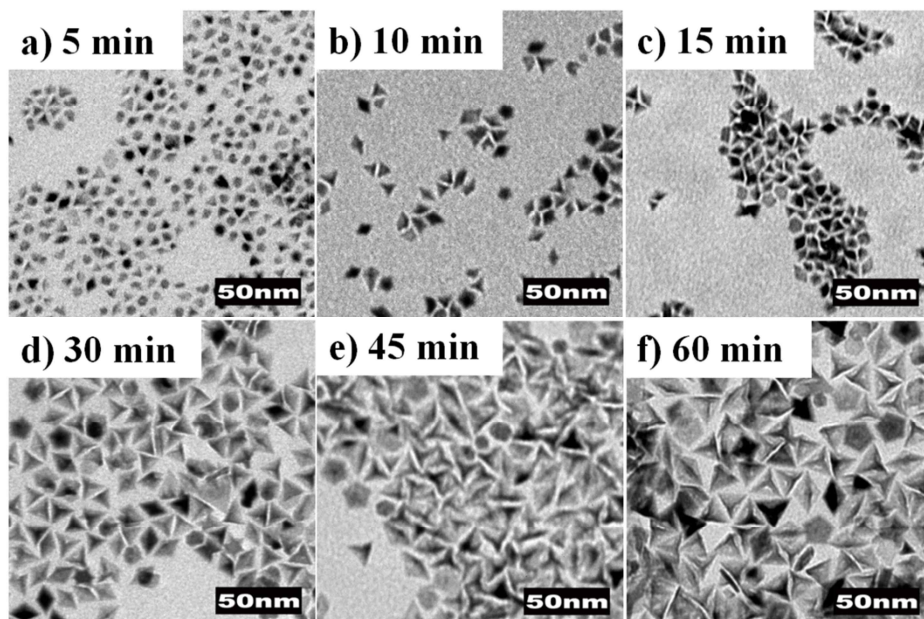
Fig. S3 a-f, Temporal TEM images of Rh tetrahedral nanoframe formation. After the initial reaction resulting Rh nanotetrahedrons, tetrahedral nanoframes were developed from the initial nanotetrahedrons.

Fig.	Reactants& Solvents					Gas	Temperature	Products
	Rh(acac)$_3$	1,2-hexadecance diol	Octadecyl amine	Stearic acid	Octadecene			
a	0.05 mmol	1.0 mmol		0.037 mmol	3 mL	under vacuum for 25 min, Ar	250 °C	Tetrahedrons & spheres
b	0.05 mmol	1.0 mmol		0.037 mmol	3 mL	under vacuum for 25 min, Ar	180 °C	No products
c	0.05 mmol	1.0 mmol		0.037 mmol	3 mL	under vacuum for 25 min, Ar	130 °C	No products
d	0.05 mmol	1.0 mmol	0.037 mmol		3 mL	under vacuum for 25 min, Ar	250 °C	Aggregated sheets & various shapes
e	0.05 mmol	1.0 mmol	0.037 mmol		3 mL	under vacuum for 25 min, Ar	180 °C	Sheets & various shapes
f	0.05 mmol	1.0 mmol	0.037 mmol		3 mL	under vacuum for 25 min, Ar	130 °C	No products
g	0.05 mmol	1.0 mmol		15.0 mmol		under vacuum for 25 min, Ar	250 °C	No product
h	0.05 mmol	1.0 mmol		15.0 mmol		under vacuum for 25 min, Ar	180 °C	No product
i	0.05 mmol	1.0 mmol		15.0 mmol		under vacuum for 25min, Ar	130 °C	No product
j	0.05 mmol	1.0 mmol	15.0 mmol			under vacuum for 25 min, Ar	250 °C	Tetrapods with a large tetrahedron on each tip & various shapes
k	0.05 mmol	1.0 mmol	15.0 mmol			under vacuum for 25 min, Ar	180 °C	Tetrapods with a small tetrahedron on each tip & various shapes
l	0.05 mmol	1.0 mmol	15.0 mmol			under vacuum for 25 min, Ar	130 °C	Tetrapods& dendrites

Table S1 The decompostion patterns of Rh(acac)$_3$ in various conditions. The increased amount of octadecylamine can decrease the decomposition temperature of Rh(acac)$_3$ while opposite is true with stearic acid. Therefore, when stearic acid was added into the reation mixture, the temperature had to be increased to form nanoparticles. Also, the presence of oxygen retards the reduction of Rh ions to Rh^0.
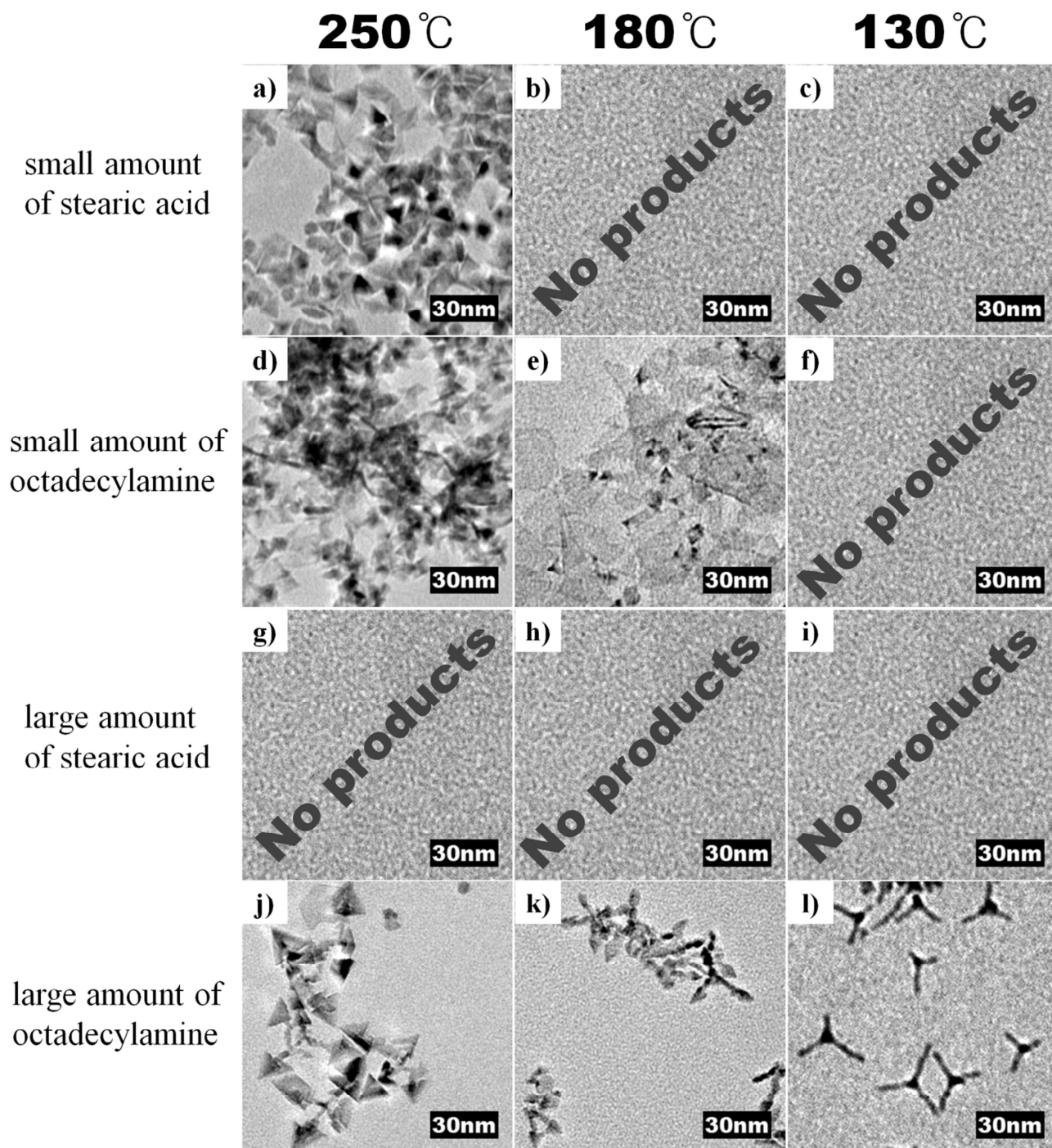
Fig. S4 Accompanied product morphologies (to Table S1). **a**, TEM image of Rh nanotetrahedrons& spheres. **d**, TEM image of aggregated Rh sheets & various shapes of Rh nanostructures. **e**, TEM image of Rh sheets & various shapes of Rh nanostructures. **j**, TEM image of Rh tetrapods with a large tetrahedron on each tip & various shapes of Rh nanostructures. **k**, TEM image of Rh tetrapods with a small tetrahedron on each tip & various shapes of Rh nanostructures. **l**, TEM image of Rh tetrapods & dendrites. **b, c, f, g, h, i**, no nanoparticle formation.
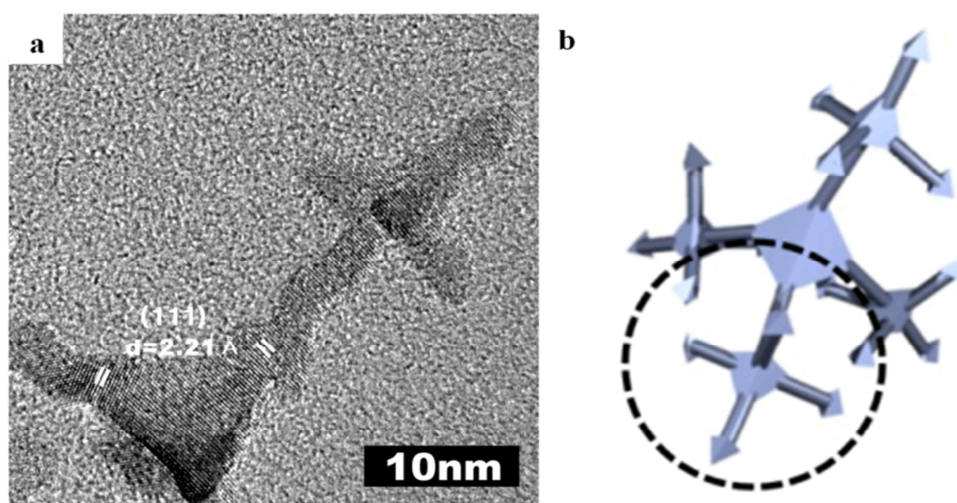
Fig. S5 a, HRTEM image of a hierarchical facet-specific Rh dendritic nanostructure (a nanotetrahedron core); the branch was developed along <111> direction. **b**, schematic model of a hierarchical facet-specific Rh dendritic nanostructure (a nanotetrahedron core).
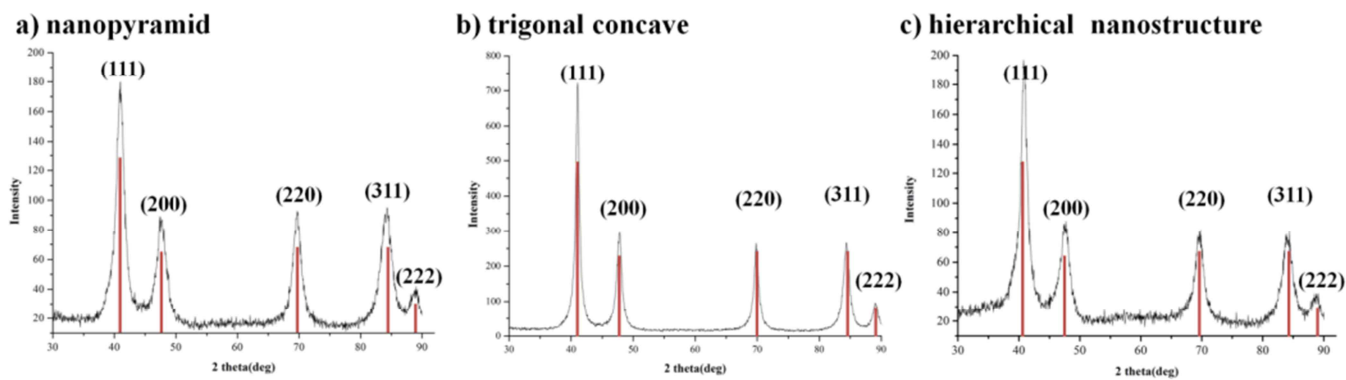
Fig. S6 X-ray diffraction patterns of Rh. **a**, nanotetrahedron. **b**, nanoframe. **c**, hierarchical dendritic nanostructures. All show that Rh exists in the same fcc phase (JCPDS card no. 71-4657).
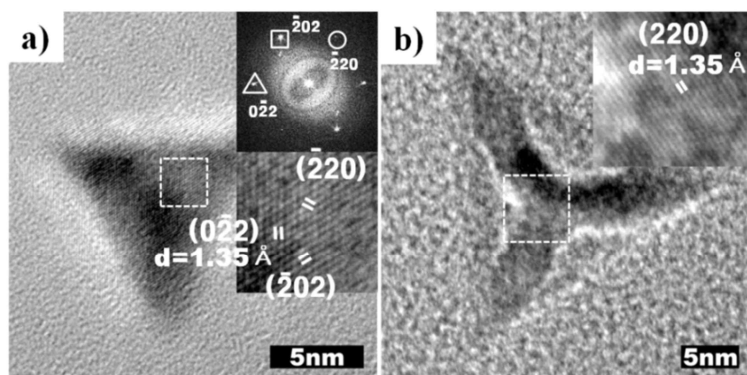
Fig. S7 HRTEM images of various Rh seed nanostructures. **a**, nanotetrahedron (single-crystalline) with FFT image of the dotted square in (**a**) along the <111> zone axis. **b**, nanoframe (single-crystalline); the 1.35 Å spacing of the lattice fringe of the dotted square in (**b**) corresponds to {220}.
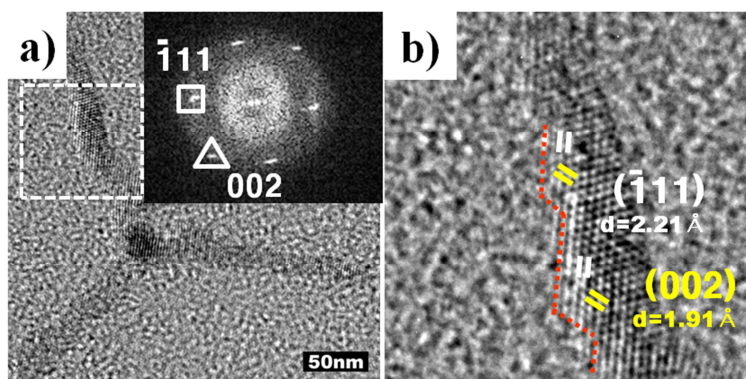
Fig. S8 HRTEM images of Rh tetrapod. **a**, Rh tetrapod with FFT image of the dotted square in the Inset. **b**, magnified image of the dotted square in (**a**). Rh arms show {100} and {111} facets in an alternating fashion (red dotted line).
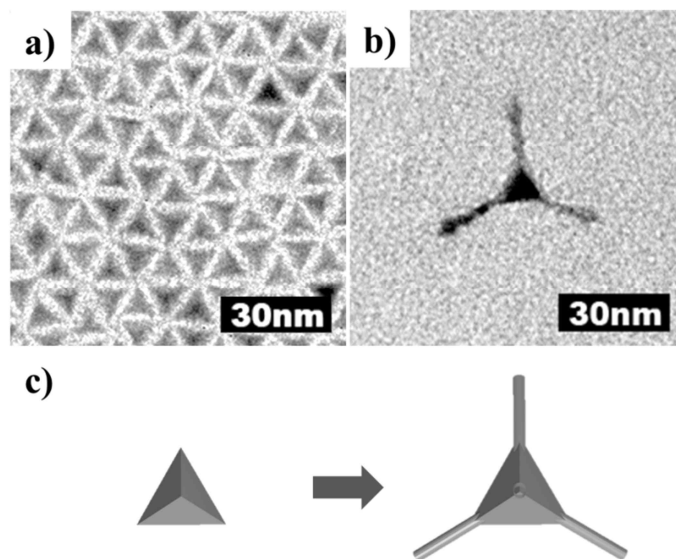
Fig. S9 TEM and schematic images of **b,** nanotetrapod arms from **a,** nanotetrahedron seed.
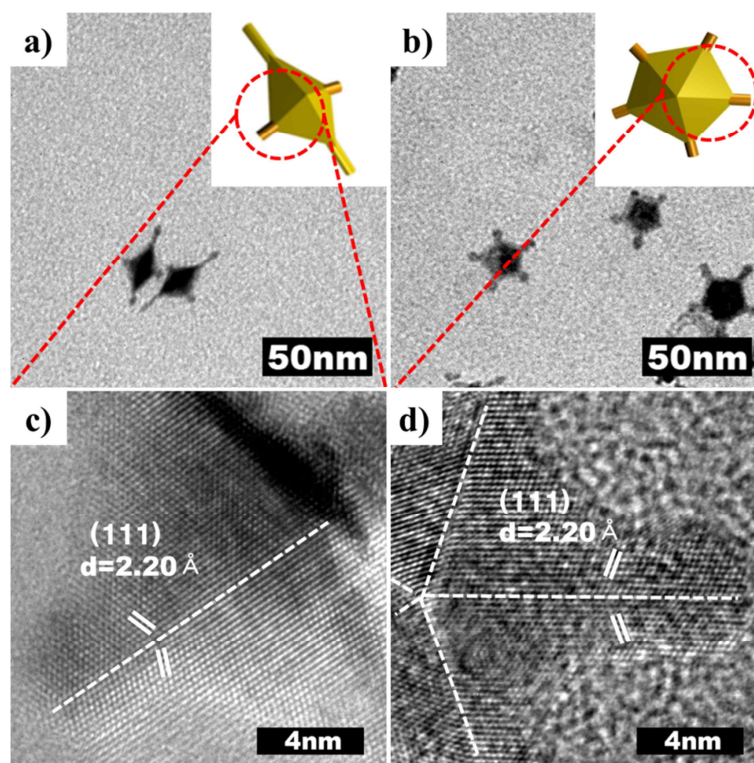
Fig. S10 TEM images of skeletal growth a, from a Rh bipyramid and b, from a Rh nanoseastar. HRTEM images of the twinned outgrown arms from c, bipyramid and d, seastar-shaped nanocrystals (Dotted line indicate grain boundaries). Note that nanotetrapods cannot be obtained by using non-tetrahedral seeds. The tetrapod formation should not occur on a seed with a different shape because the <111> direction would not pass through the crystal vertices anymore in this case.

Table S1. Comparison of catalytic activities and selectivities of Rh-based catalysts for the hydrogenation of benzo[f]quinoline.
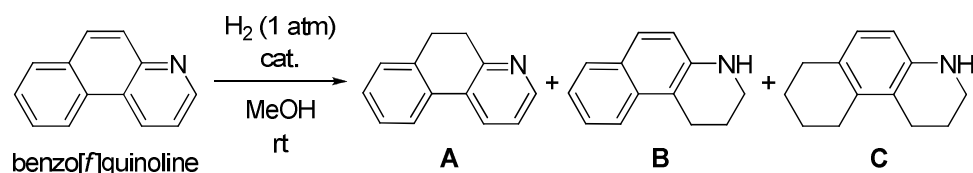
cat.[a]	mol%[b]	time (h)	conversion (%)[c]	selectivity (A : B : C)[c]
Rh/C	1.0	23	15	22 : 78 : 0
Rh-Frame	1.0	22	42	0 : 100 : 0
	2.5	20	100	0 : 100 : 0
Rh-Pyr	2.5	20	100	0 : 97 : 3
Rh-Tet	2.5	20	0	-
Rh-Dend-P	2.5	20	4.4	80 : 20 : 0
Rh-Dend-F	2.5	20	0	-

[a]Rh content of nanostructures was determined by ICP analysis: Rh-Frame 2.97wt%, Rh-Pyr[amid] 0.95wt%, Rh-Tet[rapod] 1.29wt%, Rh-Dend[rite]-P[yramid] 2.30wt%, and Rh-Dend[rite]-F[rame] 2.3wt%. The commercial Rh/C was 5wt%. [b]The mol% was calculated based on the wt% of Rh. [c]The conversion and product ratio were determined by GC-MS and compound **B** was further identified using NMR. The nanoparticles were supported on Vulcan carbon to avoid the aggregation between nanoparticles during catalysis and were placed in boiling hexane for 24 h to remove the surfactants from the nanoparticle surface. The reaction of the substrate (0.32 mmol) in MeOH (0.03 M) was carried out under 1 atm of H_2 gas at room temperature.